

# Feasibility of the Simultaneous Determination of Monomer Concentrations and Particle Size in Emulsion Polymerization Using in Situ Raman Spectroscopy

Claudia Houben,<sup>†</sup> Gabit Nurumbetov,<sup>‡</sup> David Haddleton,<sup>‡</sup> and Alexei A. Lapkin<sup>\*,†</sup><sup>†</sup>Department of Chemical Engineering and Biotechnology, University of Cambridge, Pembroke Street, Cambridge CB2 3RA, U.K.<sup>‡</sup>Department of Chemistry, University of Warwick, Gibbet Hill, Coventry CV4 7AL, U.K.

## Supporting Information

**ABSTRACT:** An immersion Raman probe was used in emulsion copolymerization reactions to measure monomer concentrations and particle sizes. Quantitative determination of monomer concentrations is feasible in two-monomer copolymerizations, but only the overall conversion could be measured by Raman spectroscopy in a four-monomer copolymerization. The feasibility of measuring monomer conversion and particle size was established using partial least-squares (PLS) calibration models. A simplified theoretical framework for the measurement of particle sizes based on photon scattering is presented, based on the elastic-sphere-vibration and surface-tension models.

## ■ INTRODUCTION

Manufacturing efficiency is a critical factor in the competitiveness of chemical industries. It includes minimal use of materials and energy per unit product or service; minimum cost of environmental remediation or waste treatment; and consistent product quality, eliminating or minimizing off-specification material. Energy efficiency and product quality are the two aspects of process performance that can be affected by improvements in process control. Understanding process behavior, implemented in a robust model, enables the maximum and safe utilization of the heating/cooling capacity of plants, and sensing and characterizing product quality during the manufacturing process enables real-time optimization of process parameters that maximize quality and throughput simultaneously. This requires implementation of real-time model-based predictive control, which, in recent years, has received a significant boost through progress in computing, modeling, sensor technologies, and chemoinformatics.<sup>1–3</sup> However, significant challenges remain in implementing model-based predictive controllers, especially in situations when product quality and/or process parameters are difficult to observe directly and require soft sensors in addition to hard sensors. Here, we define a soft sensor as a model that receives hard sensor measurements and computes parameter(s) enabling the determination of process state variables.

One such area of significant industrial interest is emulsion polymerization. Emulsion polymerization is a complex multiphase reaction. Batch or semibatch polymerization is frequently used in industry and is challenging and interesting for in situ monitoring, because of time-course variations in concentrations and the gradual change of physical properties within the system. Semibatch polymerization, typically performed in the monomer-starved regime, provides an additional challenge for in situ monitoring because of the low concentrations of the monomers. Yet, for the complete description of a reaction, it would be highly desirable to know the concentrations of all

monomers and reagents in all phases and to have real-time measurements of product quality. At a minimum, it is desirable to be able to measure the particle size distribution as a measure of product quality.

At present, it is impossible to devise a measurement technique that would determine monomer concentration in the latex phase. In situ information about an emulsion polymerization process is currently (industrially) obtained by a few hard sensors measuring the temperature, the pressure, and the flow of the cooling medium. Information about the heat balance is evaluated on the balance of these measurements. However, the polymerization rate of the monomers and the individual monomer concentrations are not observable from the overall heat rate.<sup>4</sup>

Similarly, in situ monitoring of the particle size distribution is not currently feasible at present. For particle size measurements, a few online sensors are available, such as turbidity meters, photon density wave (PDW) probes,<sup>5</sup> focused-beam reflectance measurement (FBRM) probes,<sup>6</sup> ultrasound sensors,<sup>7–9</sup> fiber-optic quasielastic light scattering (FOQLS),<sup>10,11</sup> and attenuated-total-reflection infrared (ATR-IR) spectroscopy.<sup>12–14</sup> For a critical review of different techniques for monitoring latex particles, the reader is directed elsewhere.<sup>15</sup> None of these techniques allow in situ measurements in a multiphase reaction system. Thus, at present, robust and reliable hard sensors that would provide in situ measurements of product quality in an emulsion copolymerization process do not exist.

To overcome the lack of observability, it would be highly desirable to have more in situ information. Process Raman spectroscopy is routinely used in some industries. It has already

**Received:** July 27, 2015

**Revised:** November 27, 2015

**Accepted:** December 7, 2015

**Published:** December 7, 2015

been successfully demonstrated for monitoring the conversion of individual monomers in emulsion polymerization.<sup>16–26</sup> An immersion Raman probe positioned in the bulk of a reaction mixture samples the continuous phase with dispersed particles of monomer(s) and polymer, thus providing a global measure of monomer concentration(s). The ability to measure monomer concentrations with Raman spectroscopy depends strongly on their scattering intensities and the spectral overlap between components of a reaction mixture.<sup>27,28</sup> Raman scattering data were also shown to be useful in measuring particle sizes of inorganic nanoparticles.<sup>29–31</sup> It would be beneficial to combine the ability to measure monomer concentrations and particle sizes with a single in situ probe.

Ito et al. developed a method for determining particle size during emulsion polymerization using Fourier transform (FT) Raman spectroscopy combined with multivariate data analysis.<sup>32</sup> This method was tested on different particle sizes with different monomer ratios and showed good agreement between the statistical model and the measured particle sizes. However, this method was tested offline using polymer dispersions of different sizes, rather than in a reaction. Furthermore, in a different study, a partial least-squares (PLS) model of a full spectrum (400–4000  $\text{cm}^{-1}$ ) was shown to predict particle sizes in a polymerization process.<sup>26</sup> However, it is also known that information about particle vibrations and vibrations of the chain expansion is restricted to low wavenumbers ( $<400 \text{ cm}^{-1}$ ).<sup>33,34</sup> Thus, a more detailed study of Raman scattering in emulsion polymerization is justified.

Inspired by the huge impact of the copolymerization of styrene and butyl acrylate on industry and research,<sup>35–41</sup> we studied mainly this two-monomer system. Herein, we present the feasibility of the measurement of both monomer conversion and particle size using a single immersed Raman probe in batch emulsion copolymerization. Several calibration techniques are compared for measurements of both concentration and particle size. Furthermore, we correlate predictions of particle size with spectral shift in the low-wavenumber region of Raman spectra.

## ■ EXPERIMENTAL SECTION

**Materials.** Styrene (ST, Aldrich, 98%), butyl acrylate (BA, Sigma-Aldrich, 99%), methyl acrylate (MA, Aldrich, 99%), acrylic acid (AA, Aldrich, 99%) sodium dodecylbenzenesulfonate (SDBS, Sigma, 99%), and potassium persulfate (KPS, Aldrich) were all used as received. Milli-Q-water was used in all experiments.

**Polymerization Experiments.** Polymerization was performed under a nitrogen atmosphere in a 0.5 L double-jacketed glass reactor (Radleys), equipped with a four-blade turbine impeller, set at 300 rpm in all experiments. The temperature of the reaction mixture was maintained using a Cryo-Compact Circulator (CF41 Julabo). In a typical batch experiment, the reaction temperature was 60 °C, the total amount of monomer was 15 wt %, and 3 wt % SDBS and 0.63 wt % KPS with respect to the overall amount of monomers were added. Three molar ratios between styrene and butyl acrylate (ST/BA) were used, namely, 50:50, 80:20, and 87:13, and are specified in the results. In the case of the four-monomer copolymerization, the monomer ratios were always styrene/butyl acrylate/methyl acrylate/acrylic acid = 0.73:0.18:0.05:0.05. The monomer mixture, water, and surfactant were combined and flushed with nitrogen for 1 h before being heated to the reaction temperature. After reaching the reaction temperature, the deoxygenated initiator solution was added to the reaction

mixture to start the reaction. Conversion of monomers was monitored by offline gas chromatography (GC) and in situ Raman measurements. To determine monomer conversion by GC, 0.5 mL of the reaction mixture was added to 5 mL of THF, and 0.05 mL of toluene was added as an internal standard. The sampling method ensured that all monomer was sampled regardless of its distribution between different reaction phases.

**Raman Spectrum Simulations.** Simulations of the Raman spectra of polystyrene were performed using Spartan 14 (v. 1.1.14) for oligomer chains with up to five monomer units. The calculations were carried out in the equilibrium ground-state geometry with Hartree–Fock 3-21-G in vacuum.

**Analytical Methods.** A Shimadzu gas chromatograph (GC-2014) equipped with a capillary column (FactorFour VF, 1 m for a 15-m length and 0.25-mm i.d., 0.25- $\mu\text{m}$  film thickness, Varian) and flame ionization detector was used for monitoring conversion of the monomers.

The Raman spectrometer (Horiba Jobin Yvon LabRAM HR) was equipped with an Olympus BX41 microscope ( $\times 10$  objective) and a Superhead Fiber Probe with 10-m-long fibers and a semispherical immersion probe with sampling depth of several micrometers. The instrument was calibrated using the 520.5  $\text{cm}^{-1}$  line of silicon. Raman spectra were excited by a Nd:YAG laser (532.8 nm, 16 mW) at a nominal resolution of 4–6  $\text{cm}^{-1}$  in the range between 150 and 1800  $\text{cm}^{-1}$ . The acquisition was repeated four times with an exposure time of 8 s. Repeated acquisitions were performed to improve the signal-to-noise ratio. PEEXACT software (supplied by S-Pact) was used for data analysis.

Dynamic light scattering (DLS) was measured on a Malvern Zetasizer Nano S90 instrument at a concentration of approximately 1  $\text{mg mL}^{-1}$ . Two measurements of 12 subruns each were obtained at a 173° backscatter measuring angle, equilibrated at 25 °C.

**Raman Model for Predicting Monomer Concentration.** All spectra were normalized to the intensity of the 1000  $\text{cm}^{-1}$  band to reduce the influence of phenomena other than bond formation on the Raman signal intensity. The models were calibrated on 52 spectra of different emulsion copolymerization reactions, where the monomer ratio was kept constant but the reaction temperature was varied between 60 and 90 °C to show the potential of the calibration model.

For peak integration (PI), the 1610–1690  $\text{cm}^{-1}$  peak area was chosen, which includes the vinyl groups of both styrene and butyl acrylate. Although additional areas were added to the model, no improvement was achieved, and only this spectral range was used for PI model. For the indirect hard model (IHM) and the partial least-squares (PLS) model, the entire normalized spectra were taken into account.

The indirect hard model (IHM)<sup>42</sup> was built with the pure-component spectra of styrene, butyl acrylate, and the copolymer. These pure components were described with 15–20 Lorenz peak distributions. The number of peaks was chosen depending on the error of the hard model fit to the spectra. Root-mean-square errors (RMSEs) below  $<0.1$  were considered acceptable. Table 1 reports the results of the calibration of 52 spectra compared with offline GC data. For the PLS model, a multivariate regression function was fitted to the calibration data.

**Raman Models for Predicting the Particle Size of Latex Particles.** For predicting particle size, only a statistical method, specifically the partial least-squares (PLS) model, was used. Different models were developed for comparison. The

**Table 1. Results of Validation of the Different Models for Prediction of the Overall and Individual Monomer Concentrations**

		calibration $R^2$	RMSECV <sup>a</sup>	function/rank
model 1	PI (overall)	0.97	6.55	linear
model 2	IHM (overall)	0.95	8.12	linear
model 3	PLS (overall)	0.98	6.13	4
model 4	IHM (ST)	0.98	5.74	linear
model 5	IHM (BA)	0.64	22.96	linear
model 6	PLS (ST)	0.98	6.23	4
model 7	PLS (BA)	0.97	7.79	4

<sup>a</sup>Root-mean-square error of cross-validation.

first model, model 8, considered the spectral range of 150–400  $\text{cm}^{-1}$  and included a baseline correction with a linear-fit subtraction. For model 9, the same spectral range, 150–400  $\text{cm}^{-1}$ , was used, but it was normalized to the intensity of 1000  $\text{cm}^{-1}$  band. Models 10 and 11 considered the entire spectrum between 150 and 1800  $\text{cm}^{-1}$ . Model 10 included a linear baseline correction, whereas model 11 additionally used normalized spectra. The results of validation of the methods are reported in Table 2.

## RESULTS AND DISCUSSION

**Monomer Concentration Monitoring with in Situ Raman.** In the case of the copolymerization of styrene and butyl acrylate, the stretching vibrations of the vinyl group in the two monomers appear at 1631 and 1639  $\text{cm}^{-1}$ , respectively.<sup>43</sup> As a result of this overlap, the band corresponding to the vinyl group cannot be associated with a specific monomer. Furthermore, butyl acrylate does not have many other significant bands (see Supporting Information, Figure S1). When used in a styrene/butyl acrylate molar ratio of 80:20 or greater, the determination of butyl acrylate by Raman spectroscopy is problematic because of a low signal intensity and significant spectral overlap.

Spectral overlap and low scattering, leading to significant errors in quantitative concentration determinations, are well-known problems of in situ optical spectroscopy. In the case of emulsion polymerization, an additional complication is the observed decrease in intensity of the entire spectrum in the early phase of reaction (see Supporting Information, Figure S2). Such a decrease was reported earlier<sup>16,18,44</sup> and was linked to the onset of polymerization, or less light being collected because of scattering by forming and growing latex particles. However, for the determination of monomer concentrations, the effect of variable scattering is detrimental and, therefore, was eliminated by normalizing the overall spectra to the intensity of the 1000  $\text{cm}^{-1}$  band, corresponding to the breathing mode of the phenyl group.

For the prediction of monomer concentrations, three different methods were used initially: peak integration (PI),

partial least-squares (PLS), and indirect hard modeling (IHM). The peak integration model was able to predict only the overall conversion and was found to be unreliable in predicting the concentration of each monomer because of the high spectral overlap. However, to increase the observability of the system, it is unsatisfactory to estimate the overall conversion alone. Rather, it is highly desirable to quantify the concentrations of the individual monomers.

The PLS model was found to slightly underestimate the conversions of the monomers at the beginning of the reaction but to fit well the offline measurements toward the end of the reaction (see Figure 1). In the first few minutes of a reaction after addition of the initiator, the process is influenced by nucleation, the shrinking of the monomer droplets, and the formation of particles. Although the spectra were normalized to decrease this effect, the disturbance introduced by the rapid change in the physical properties of the system apparently translates into errors in the quantification of concentrations at the beginning of the reaction.

The IH model was found to poorly describe the concentration profile of butyl acrylate (Figure 2). This model was built from the spectra of all three components: styrene, butyl acrylate, and copolymer. Butyl acrylate has no significant peaks in the spectrum of the reaction mixture. In addition, the low ratio of butyl acrylate in the studied system further reduced the accuracy of its quantification. As a result, IHM overestimates the concentration of butyl acrylate at the beginning of polymerization. Of particular interest in IHM is the adjustment of the component weight parameters based on the analysis of the concentration of each component. This is done by model fitting. Each model parameter is automatically adjusted until the hard model fits a certain measured spectrum.<sup>42</sup> However, normalization might affect the weighting of the single spectra and might be one reason for the poor prediction of the butyl acrylate concentration.

In the case of the emulsion copolymerization of styrene and butyl acrylate, the PLS model describes the conversions of the two monomers better than the IHM. However, in general, PLS models are limited to their calibration range. In the case of such a complex process as emulsion polymerization, changes in process conditions or composition, such as substitution of the surfactant or monomers, would require retraining of the PLS calibration model to enable in situ monitoring of the monomers.

To investigate the robustness of the obtained PLS calibration model for monomer concentrations, predictions of the concentrations were performed with PLS models calibrated with data obtained at different monomer ratios. Thus, predictions of the concentrations in an experiment with a styrene/butyl acrylate ratio of 80:20 were performed with a PLS model calibrated on the data obtained with a 50:50 monomer ratio, and vice versa. These experiments also tested the significance of intermolecular interactions within this

**Table 2. Details of Different PLS Models Used to Predict Particle Size in the Emulsion Copolymerization of Styrene and Butyl Acrylate**

range data treatment	model 8 150–400 $\text{cm}^{-1}$ baseline correction	model 9 150–400 $\text{cm}^{-1}$ baseline correction, normalization	model 10 150–1800 $\text{cm}^{-1}$ baseline correction	model 11 150–1800 $\text{cm}^{-1}$ baseline correction, normalization
rank	5	4	4	4
$R^2$	0.74	0.73	0.68	0.66
RMSECV	18.13	17.84	17.40	18.10

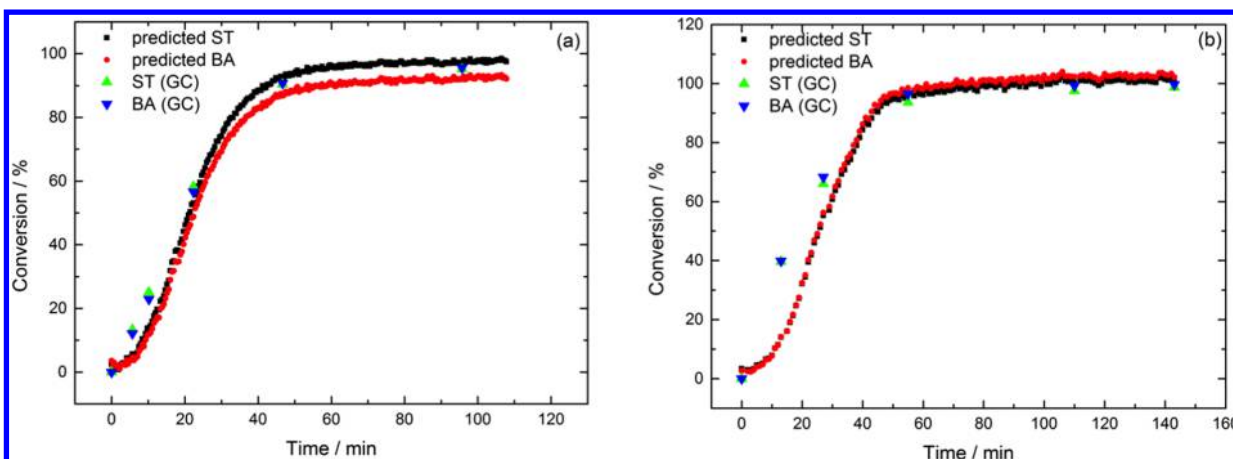


**Figure 1.** Conversions of styrene and butyl acrylate for ST/BA monomer ratios of (a) 80:20 and (b) 87:13 predicted using the PLS model compared with offline GC data.

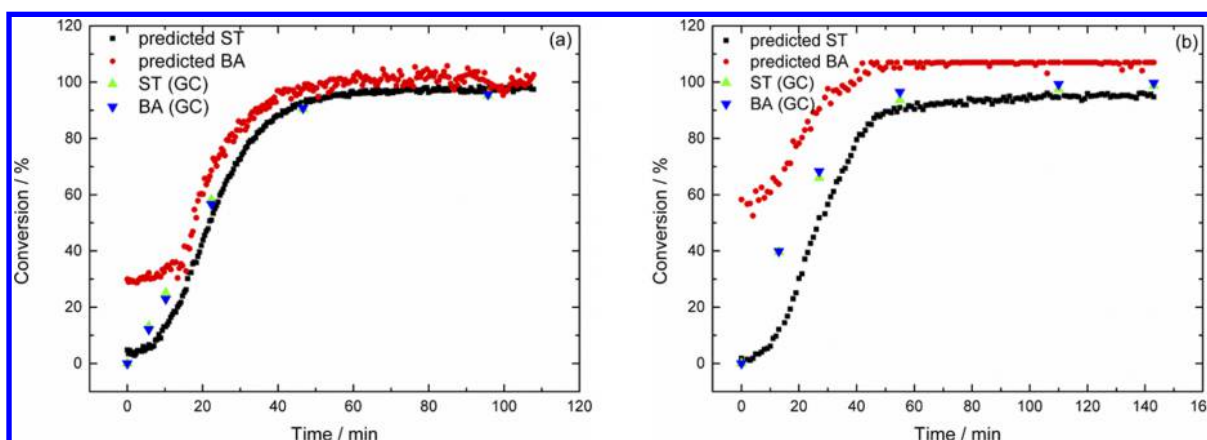


**Figure 2.** Conversions of styrene and butyl acrylate for ST/BA monomer ratios of (a) 80:20 and (b) 87:13 predicted using the IH model compared with offline GC data.

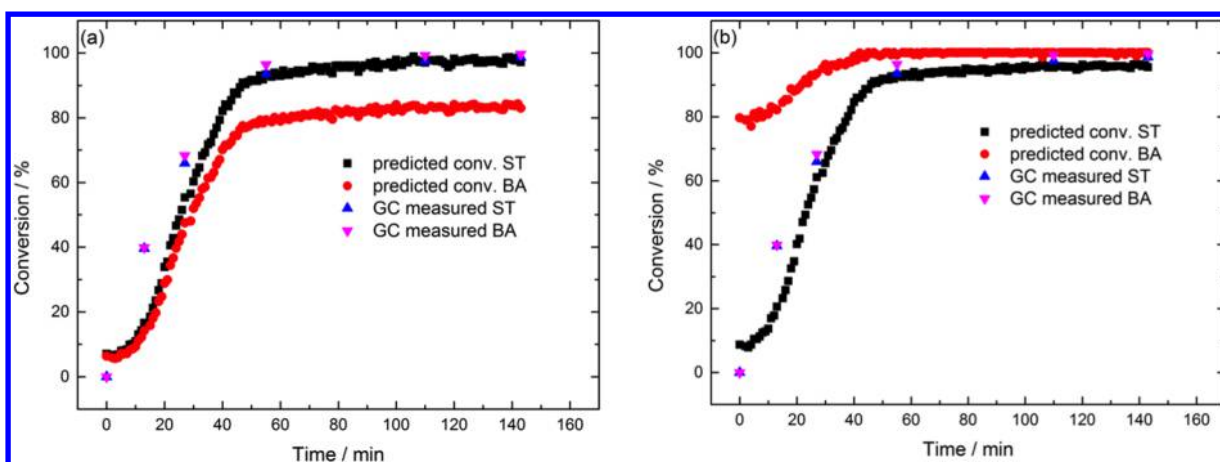


**Figure 3.** Prediction of conversion in an experiment using a 80:20 styrene/butyl acrylate monomer ratio using models calibrated on a 50:50 monomer ratio: (a) PLS model and (b) IHM.

system in PLS calibration models. IH models were tested in the same manner for completeness.

Figure 3 shows the predictions of the polymerization reaction for the monomer ratio of 80:20 with a model calibrated for a 50:50 ratio. These predictions are surprisingly good for a model not trained on the specific monomer ratio: The PLS model describes the conversion profile well, whereas IHM does not

predict the butyl acrylate concentration. The same was done in reverse, with a model calibrated on the 80:20 training data used to predict the conversions in an experiment with a 50:50 monomer ratio, and good agreement was found (Supporting Information, Figure S11). However, the predictions of the conversions at the start of the reaction were slightly deteriorated compared to those of models trained on the

correct monomer ratios (see Figure 1). This still implies the need for more extensive model calibration at the early stages of the reaction and for the specific monomer ratios.

A good prediction by a statistical model outside its calibration range suggests a low contribution of intermolecular interactions to the spectra. Such interactions would normally make it impossible to extend the range of a statistical model beyond its training set.

A system more relevant to many industrial polymerization processes would involve more than two monomers, for example, a four-monomer system. We evaluated the feasibility of developing a spectral calibration model for a four-monomer system including acrylic acid, methyl acrylate, styrene, and butyl acrylate. The individual spectra of the pure monomers are shown in Figure 4.

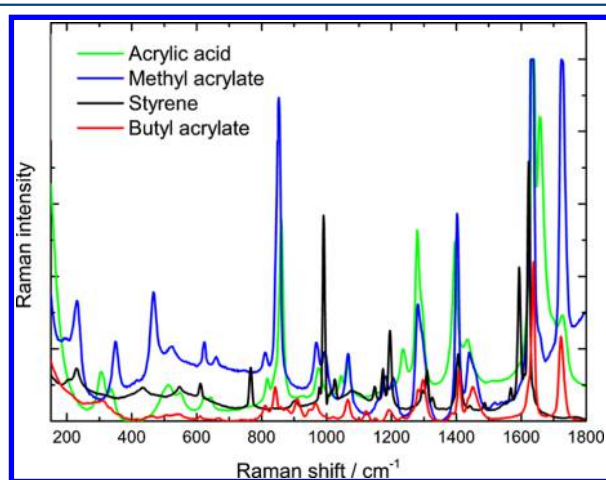


Figure 4. Pure Raman spectra of the four-monomer system.

The similar structures of the acrylic monomers chosen for the four-monomer system are reflected in the Raman spectra. The overlapping of the bands is significant and results in a highly inaccurate prediction model. For industrial relevance, the amounts of the water-soluble monomers, acrylic acid and methyl acrylate, should remain at <8 wt %. At such low concentrations of the water-soluble monomers, we were unable to develop calibration models for these monomers, because of low signal-to-noise ratios and significant overlap of key bands.

Hence, predictions of the conversions of the individual monomers in this system by Raman spectroscopy still remain challenging. Only the overall conversion was predicted, as shown in Figure 5.

In comparison with an IH model, prediction of the overall conversion is better served with the PLS calibration model. Although IHM is a powerful technique for predicting conversion, it appears to be unsuitable for this specific system with significant spectral overlap.<sup>42</sup> The PLS model does not rely on a mechanistic description of the spectra and allows one to achieve better predictions of monomer concentrations despite low signal-to-noise ratios.

**Online Monitoring of Particle Size Based on Raman Spectroscopy.** The observed decrease in intensity of the overall spectra in the early stages of the polymerization reaction is associated with some physical changes in the reaction mixture and might allow for a correlation with particle size by either direct or indirect methods. Possible mechanisms behind the intensity suppression are turbidity, refractive index, and increasing scattering due to the formation and growth of particles. The latter possibility is the basis for an examination of whether a single Raman immersion probe could be used to monitor both the concentration of monomers and the particle size of the product polymer.

**PLS Model to Predict Particle Size.** Several PLS models were developed using different spectral ranges and different spectral corrections. The first model (model 8) included the range of 150–400  $\text{cm}^{-1}$  and correction of the baseline with a linear-fit subtraction. For model 9, the same spectral range (150–400  $\text{cm}^{-1}$ ) was taken into account, but this time the spectra were normalized to the band at 1000  $\text{cm}^{-1}$ . Models 10 and 11 included the entire spectral range (150–1800  $\text{cm}^{-1}$ ). The differences between these models were that model 10 corrected the baseline with a linear-fit subtraction and model 11 also used normalized spectra.

Figure 6 shows the particle size in an emulsion copolymerization reaction predicted by all four models and the corresponding offline DLS measurements. These experiments were performed with the four-monomer system. Taking the entire untreated spectrum into account (150–1800  $\text{cm}^{-1}$ ), model 10 gave a significant error in particle size prediction ( $R^2 = 0.68$ ). Using the normalized spectra for the calibration, model 11 gave a slightly higher error ( $R^2 = 0.66$ ). The reason for this

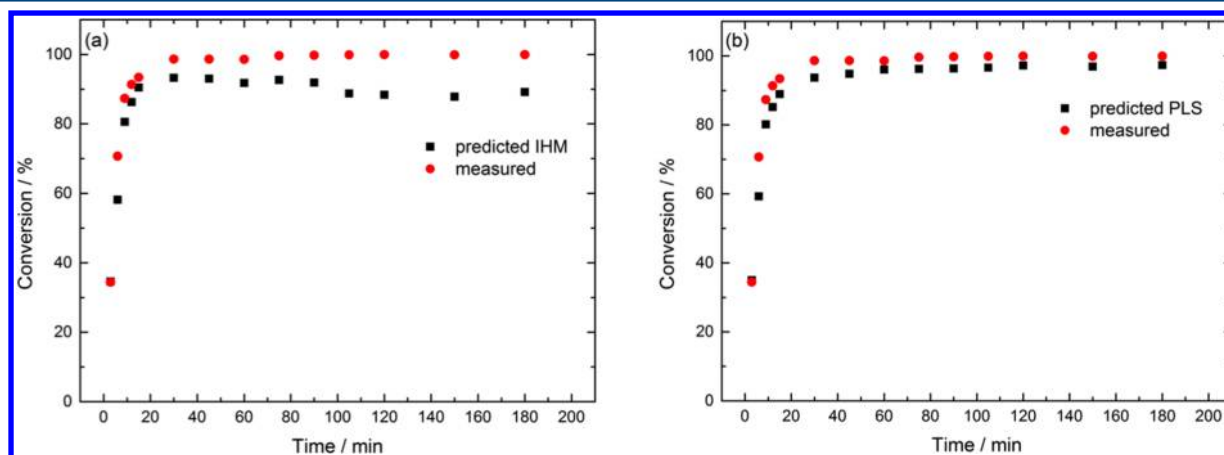
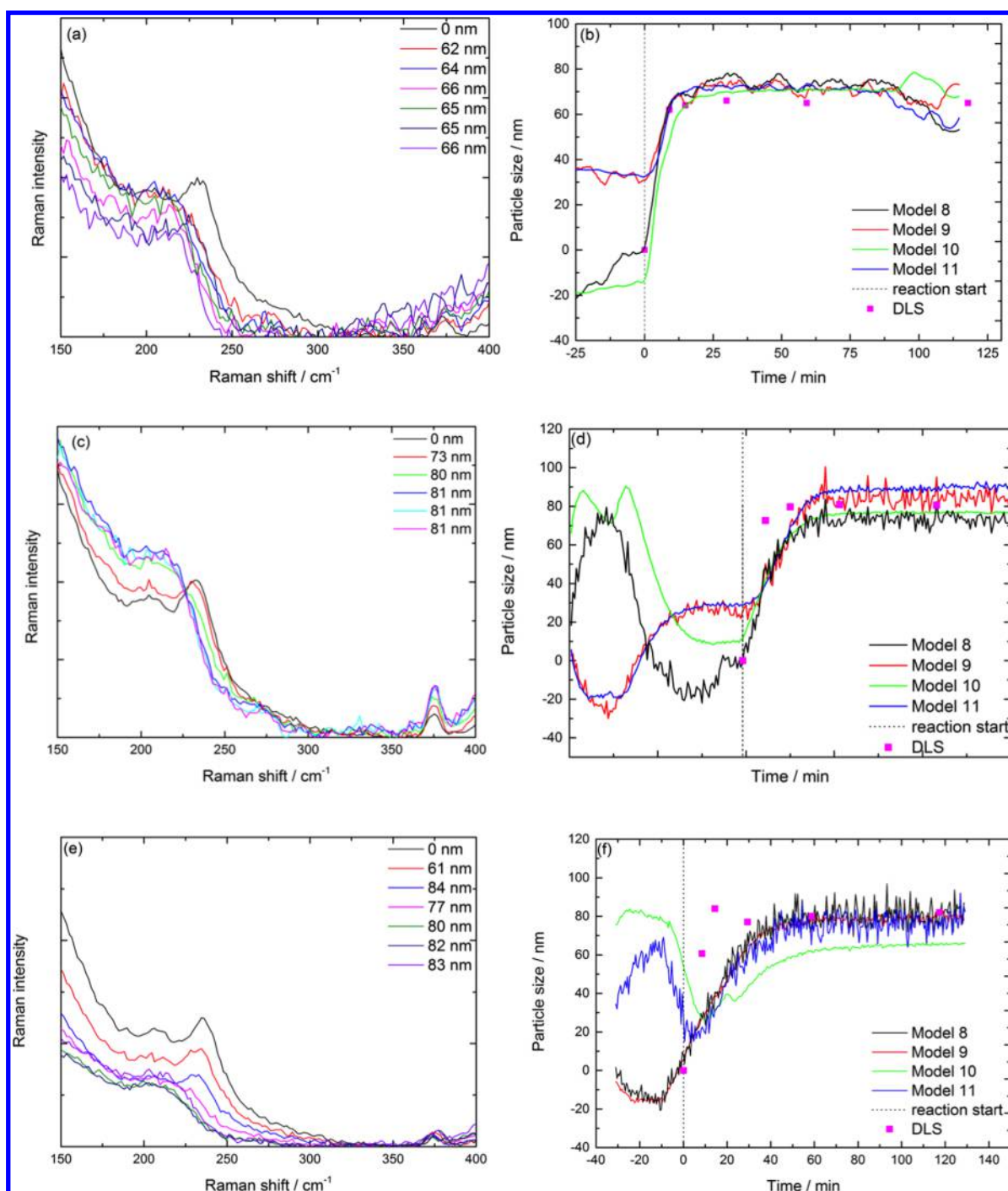


Figure 5. Overall conversions of emulsion copolymerization predicted with (a) IHM and (b) PLS model for the four-monomer copolymerization. The predicted values were obtained by Raman spectroscopy, and the measured values were obtained by offline GC analysis.



**Figure 6.** (b,d,f) Predictions of average particle size using different PLS models compared with offline DLS measurements for different experiments. (a,c,e) Changes in Raman intensity at low wavelength corresponding to the performed experiments. All experiments performed with the four-monomer system. Experiments corresponding to graphs a,b and c,d were performed at 60 °C, and experiment corresponding to graphs e,f was performed at 80 °C.

is that the effect of growth in particle size is partially filtered out by normalization. In both cases, the PLS model had rank 4, which indicates the complexity of the model, but was not too high to overestimate the correlation between the particle size and Raman spectra.

It is known that, at low wavenumbers, vibrations of elastic spheres and chain-expansion vibrations can be observed.<sup>33</sup> Therefore, PLS models were built focusing on this region (150–400 cm<sup>-1</sup>). As expected, the PLS models for both the treated (model 9) and untreated (model 8) spectra exhibited

much better results than the models that included the entire spectral range (Table 3).

It can be seen that, at the start of the reaction, the models struggled to estimate particle size. This is not surprising given that, at the beginning of a reaction, the emulsion solution consists of monomer droplets, surfactant, and water but no polymer particles. The standard DLS instrument used in this study is capable of measuring particle sizes in the range from 0.3 nm to 10 μm. The beginning of the reaction ( $t = 0$ ) was defined as zero particles ( $d = 0$ ) for the Raman calibration set.

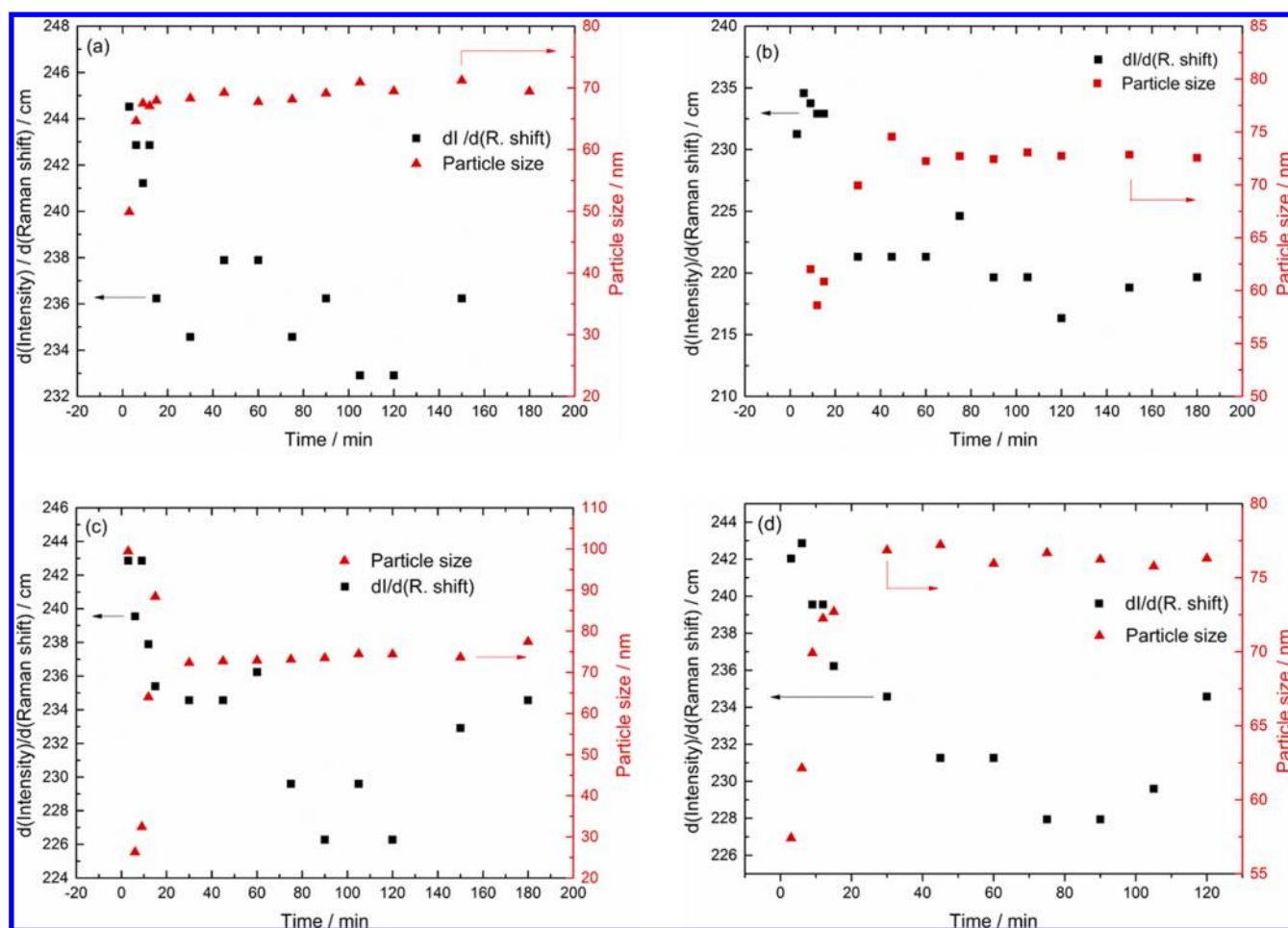


**Figure 7.** Comparison of offline measured particle size (red) and peak shift (black) during different experiments performed with the two-monomer system. ST/BA monomer ratios of (a) 80:20 at 80 °C, (b) 50:50 at 60 °C, (c) 50:50 at 60 °C, and (d) 80:20 at 70 °C.

However, Figure 6 shows that, although the models were trained for zero particles, the models misinterpreted the scattering that occurred prior to nucleation. The discrete behavior of emulsion polymerization might cause problems for a statistical model, such as rapid changes in the number of particles at the beginning of the polymerization followed by much slower growth of the particles, which appears to be predicted rather well. The rapid changes within the polymerization reactor at the start of the reaction give rise to multiple scattering phenomena, which introduce errors in the linear regression model. Validation of the calibration models does show high error for the prediction of zero particles (Supporting Information, Figure S14).

Nevertheless, a PLS model can be used as a fast and reasonably accurate method of monitoring particle sizes during emulsion polymerization within the validity of the PLS model calibration set. Because the PLS models were also more accurate in predicting monomer concentrations, a single type of spectral model with two different calibration sets can be used to simultaneously measure monomer concentration and particle size.

**Elastic-Sphere and Surface-Tension Models to Predict Particle Size with Raman Spectroscopy.** Predictions of particle size with Raman spectroscopy would be even more robust and accurate if scattering could be described with a physical model. As known from the literature, at low wavenumbers, acoustic vibrations of elastic spheres can be

observed.<sup>45</sup> The frequency shift of these vibrations depends on the size of the elastic spherical particle. The possibility of observing such frequency shifts in Raman spectroscopy is well-established, and phonon-confinement or elastic-sphere models are used to determine particle size. A detailed overview of this application was published by Gouadec and Colombar.<sup>31</sup>

It has also been stated that, in the low-wavenumber region ( $<400\text{ cm}^{-1}$ ), chain-expansion vibrations can be observed.<sup>46</sup> These are bending vibrations in which all C–C–C angles are changed in phase, resulting in the overall expansion and contraction of the aliphatic backbone. These Raman bands are typically observed around  $400\text{ cm}^{-1}$ , for example, ca.  $370\text{ cm}^{-1}$  for *n*-pentane and  $250\text{ cm}^{-1}$  for *n*-hexane. Simulations of Raman vibrations for styrene oligomers (see Supporting Information) have shown that chain-extension vibrations are in the range of  $200\text{--}400\text{ cm}^{-1}$ , that is, in the range observable with a typical spectrometer. This might be the phenomenon that gives rise to the observed variations in the spectra in this work (see Figures 6–8). However, at this stage, we have not developed a physical model linking chain-extension vibrations to particle size.

The changes in Raman spectra occurring during a polymerization reaction involve not only changes in intensity, as discussed above and used in statistical PLS models, but also shifts in the peak position at low wavenumbers (see Figure 7). Plotting the Raman shift against the reaction time and overlaying this plot with the change in particle size reveals a

trend. With increasing particle size, the Raman intensity shifts to lower wavenumbers. After a reaction time of about 20 min, the chain-extension vibration does not change much, and its peak scatters at about  $236 \pm 2 \text{ cm}^{-1}$ . This corresponds to the observed conversion profile: At high conversions, the mean particle size no longer changes significantly.

We observed experimentally the shift in position of Raman bands as a function of time, or reaction progress, during emulsion copolymerization (Figure 8). Looking for theoretical

**Table 3. Use of the Elastic Sphere Model to Calculate the Raman Shifts of the Elastic-Sphere Vibration for Different Sphere Sizes**

R (nm)	$\omega_s \text{ (s}^{-1}\text{)}$	$k \text{ (cm}^{-1}\text{)}$
1	$5.4 \times 10^{12}$	1129
10	$5.4 \times 10^{11}$	113
20	$2.7 \times 10^{11}$	56
30	$1.8 \times 10^{11}$	38
40	$1.4 \times 10^{11}$	28
50	$1.1 \times 10^{11}$	23
100	$5.4 \times 10^{10}$	11

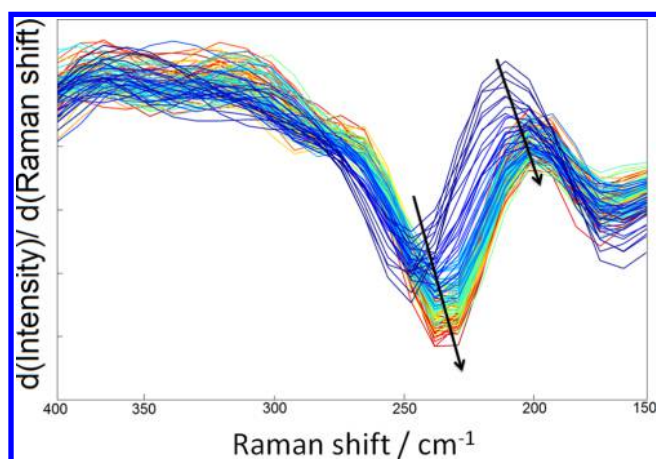


**Figure 8.** Variations in Raman shift as a function of reaction time.

foundations for the shift in Raman peak intensity, we considered two simple models, namely, the elastic-sphere model and surface-tension model, to calculate the vibrations of a spherical particle that could give rise to a Raman shift.

The equation for the frequency,  $\omega$ , of an elastic sphere was derived elsewhere as<sup>47</sup>

$$\omega_s = \omega_0 [2(2l + 1)(l - 1)]^{1/2} \quad (1)$$

with  $\omega_0^2 = \mu/(\rho_0 R^2)$ , where  $\mu$  and  $\rho_0$  are the shear modulus and bulk density, respectively. Equation 1 has been found to provide good experimental agreement for spherical clusters with particle diameters of  $R \approx 10\text{--}20 \text{ nm}$  irradiated by infrared laser light with a wavelength  $\lambda \approx 500 \text{ nm}$ .<sup>47</sup> The equation was derived from a continuum approach applied to the problem of normal elastic vibrations of a macroscopically small spherical particle. Equation 1 cannot be used for monopole excitation ( $l = 0$ ) because the assumption of negligible fluctuations in density was considered. The dipole field ( $l = 1$ ) of poloidal displacements contributes only to the parameter of inertia, whereas the restoring force (the parameter of stiffness) of the vibration is canceled. Therefore, the lowest multipole degree of a spheroidal mode is the quadrupole ( $l = 2$ ).

Considering only quadrupolar vibrations ( $l = 2$ ) of polystyrene particles with  $\mu = 3 \times 10^9 \text{ kg m}^{-1} \text{ s}^{-2}$ ,  $\rho = 1040 \text{ kg m}^{-3}$ , and  $R = 50 \times 10^{-9} \text{ m}$ , the frequency is given by

$$\omega_s^2 = \frac{\mu}{\rho_0 R^2} [2(2l + 1)(l - 1)] \quad (2)$$

yielding

$$\omega_s = 1.1 \times 10^{11} \text{ s}^{-2} \quad (3)$$

To calculate the wavenumber, we assumed that the phase velocity was equal to the speed of light in vacuum and that the wavenumber was equal to

$$k = \frac{2\pi\omega}{c} = \frac{2\pi \times 1.1 \times 10^{11} \text{ s}^{-1}}{2.99 \times 10^8 \text{ m s}^{-1}} = 23 \text{ cm}^{-1} \quad (4)$$

Thus, a polystyrene sphere of 100-nm diameter will vibrate at  $k = 23 \text{ cm}^{-1}$ . This vibration is too low to be detected by our Raman spectrometer because of overlap with the Rayleigh wing. The instrument used in the present study can measure Raman shifts of at least  $50 \text{ cm}^{-1}$ . The experimentally observed shifts are in the range of  $200\text{--}250 \text{ cm}^{-1}$  and cannot be explained by the vibrations of a sphere in the quadrupolar state.

To test whether the observed peak shift to lower wavenumber can be explained by the elastic sphere model, we calculated Raman shifts as a function of particle size using the elastic sphere model (Table 3). The sphere model predicts a vibrational shift to lower wavenumbers with increasing particle size. This trend was also obtained experimentally. However, the ranges of the vibrations were rather different between the model and experiment.

**Determination of Particle Vibrations with the Surface-Tension Model.** Lamb<sup>45</sup> proposed that the frequency of a resonant mode of shape oscillation for a free inviscid liquid droplet in air with axial symmetry can be expressed as

$$\omega_L^2 = \frac{l(l + 2)(l - 1)\gamma}{\rho R^3} \quad (5)$$

where  $\omega$  is the frequency,  $l$  is the mode number/resonant mode,  $\rho$  is the density,  $R$  is the equilibrium radius, and  $\gamma$  is the surface tension. Although eq 5 considers a free inviscid liquid droplet in air, the equation can be applied to our system for a rough estimation of the region where the particle vibration should be. The resonant mode is  $l = 2$ , which is, as mentioned earlier, a Raman-active mode. Other values for the calculation are the density ( $\rho = 1040 \text{ kg m}^{-3}$ ), particle size ( $R = 50 \text{ nm}$ ), and surface tension ( $\gamma = 10 \text{ mN m}^{-1}$ ).

The result for the frequency using the given values is

$$\omega_L^2 = \frac{2(2 + 2)(2 - 1)10 \text{ mN/m}}{(1040 \text{ kg/m}^3)(50 \text{ nm})^3} = 6.2 \times 10^{17} \text{ s}^{-2} \quad (6)$$

To obtain the wavenumber  $k$ , the frequency should be divided by the speed of light, giving

$$k = \frac{2\pi\omega_L}{c} = 0.16 \text{ cm}^{-1} \quad (7)$$

The estimated range for the vibration of a spherical particle is too close to the laser line to be detected by most Raman spectrometers. Thus, to date, we cannot accurately correlate the observed shift in Raman spectra at  $240 \text{ cm}^{-1}$  with a specific chain-expansion mode and particle size. Nor can we find



another fundamental scattering mechanism to predict Raman shifts as a function of particle size.

## CONCLUSIONS

In this work, we have shown the possibility of increasing the observability in a batch copolymerization process by employing a fiber-optic immersion Raman probe. We have shown that this technique can be used for monitoring the conversions of individual monomers in reasonably complex comonomer systems, or at least the overall conversion, using statistical PLS calibration models. It is also feasible to develop a PLS model for monitoring particle sizes using the low-wavenumber spectral range. This shows the feasibility of monitoring both conversion and particle size using a single physical probe. There remain limitations for spectroscopic techniques in the case of low concentrations of monomers and complex monomer mixtures.

We have identified that the observed shift in Raman spectra in the range of 200–250  $\text{cm}^{-1}$  correlates with the chain expansion vibration. However, we were unable to find a first-principles model to correlate the particle size with the observed Raman shifts. Further work on developing such a physical model is warranted.

## ASSOCIATED CONTENT

### Supporting Information

The Supporting Information is available free of charge on the ACS Publications website at DOI: 10.1021/acs.iecr.5b02759.

Raman spectra of pure styrene and butyl acrylate, 3D plots of untreated and normalized Raman spectra collected during a copolymerization reaction, parity plots for the prediction of the overall conversion and individual monomer conversions, validation of the IHM and PLS calibration models, cross-validation of the conversion predictions, model validation for particle size, and list of simulated Raman modes (PDF)

## AUTHOR INFORMATION

### Corresponding Author

\*E-mail: aal35@cam.ac.uk. Fax: +44 1223 334796.

### Notes

The authors declare no competing financial interest.

## ACKNOWLEDGMENTS

The research leading to these results received funding from the European Research Council under the European Union's Seventh Framework Programme (EC FP7) Grant Agreement NMP2-SL-2012-280827, and the Engineering and Physical Sciences Research Council under Grant EP/L003309/1. We acknowledge the contribution of Prof. Eugene Terentjev to discussions of the theory of elastic scattering.

## REFERENCES

- (1) Hergeth, W.-D. On-Line Monitoring of Chemical Reactions. In *Ullmann's Encyclopedia of Industrial Chemistry*; Wiley: Weinheim, Germany, 2006.
- (2) Frauendorfer, E.; Wolf, A.; Hergeth, W.-D. Polymerization Online Monitoring. *Chem. Eng. Technol.* **2010**, *33*, 1767–1778.
- (3) Frauendorfer, E.; Hergeth, W.-D. Industrial Polymerization Monitoring. *Macromol. Symp.* **2011**, *302*, 1–5.

- (4) Elizalde, O.; Azpeitia, M.; Reis, M. M.; Asua, J. M.; Leiza, J. R. Monitoring Emulsion Polymerization Reactors: Calorimetry Versus Raman Spectroscopy. *Ind. Eng. Chem. Res.* **2005**, *44*, 7200–7207.

- (5) Bressel, L.; Hass, R.; Reich, O. Particle sizing in highly turbid dispersions by Photon Density Wave spectroscopy. *J. Quant. Spectrosc. Radiat. Transfer* **2013**, *126*, 122–129.

- (6) Hukkanen, E. J.; Braatz, R. D. Measurement of particle size distribution in suspension polymerization using in situ laser back-scattering. *Sens. Actuators, B* **2003**, *96*, 451–459.

- (7) Challis, R. E.; Povey, M. J. W.; Mather, M. L.; Holmes, A. K. Ultrasound techniques for characterizing colloidal dispersions. *Rep. Prog. Phys.* **2005**, *68*, 1541–1637.

- (8) McClements, D. J.; Povey, M. J. W. Scattering of ultrasound by emulsions. *J. Phys. D: Appl. Phys.* **1989**, *22*, 38–47.

- (9) Carson, G.; Mulholland, A. J.; Nordon, A.; Tramontana, M.; Gachagan, A.; Hayward, G. Particle sizing using passive ultrasonic measurement of particle-wall impact vibrations. *J. Sound Vib.* **2008**, *317*, 142–157.

- (10) Wiese, H.; Horn, D. Fiber-Optic Quasielastic Light Scattering in Concentrated Dispersions: The On-Line Process Control of Carotenoid Micronization. *Berg. Bunsenges. Phys. Chem.* **1993**, *97*, 1589–1597.

- (11) Herzog, B.; Katzenstein, A.; Quass, K.; Stehlin, A.; Luther, H. Physical properties of organic particulate UV-absorbers used in sunscreens: I. Determination of particle size with fiber-optic quasi-elastic light scattering (FOQELS), disc centrifugation, and laser diffractometry. *J. Colloid Interface Sci.* **2004**, *271*, 136–144.

- (12) Yoshidome, T.; Fukuyama, N.; Fukushima, Y.; Higo, M. Determination of particle size by using incidence-angle dependence of spectral intensity for particle-size-measurement method by applying infrared attenuated-total-reflection technique and its simulations by using algebraic-simultaneous equations. *Anal. Sci.* **2008**, *24*, 939–943.

- (13) Yoshidome, T.; Fukushima, Y.; Higo, M. Theoretical treatment of particle-size measurements by applying attenuated-total-reflection technique and its comparisons with experimental results. *Anal. Sci.* **2008**, *24*, 443–449.

- (14) Sarno, B. J.; Yoshidome, T.; Ikuta, Y.; Rabor, J. B.; Tsurumura, Y.; Montecillo, M. E.; Higo, M. Application of Infrared Attenuated Total Reflection Technique combined with Sedimentation Phenomena to Particle Size Measurement: Fundamental Experiments on Applicability of the Method. *J. Appl. Spectrosc.* **2013**, *80*, 482–485.

- (15) Hass, R.; Munzke, D.; Reich, O. Inline-Partikelgrößenmesstechniken für Suspensionen und Emulsionen. *Chem. Ing. Tech.* **2010**, *82*, 477–490.

- (16) McCaffery, T. R.; Durant, Y. G. Application of low-resolution Raman spectroscopy to online monitoring of miniemulsion polymerization. *J. Appl. Polym. Sci.* **2002**, *86*, 1507–1515.

- (17) McCaffery, T. R.; Durant, Y. G. Monitoring of Seeded Batch, Semi-batch, and Second Stage Emulsion Polymerization by Low Resolution Raman Spectroscopy. *Polym. React. Eng.* **2003**, *11*, 507–518.

- (18) Van den Brink, M.; Pepers, M.; van Herk, A. M.; German, A. L. Emulsion (Co) Polymerization of Styrene and Butyl Acrylate Monitored by On-line Raman Spectroscopy. *Macromol. Symp.* **2000**, *150*, 121–126.

- (19) Van den Brink, M.; Pepers, M.; van Herk, A. M. Raman spectroscopy of polymer latexes. *J. Raman Spectrosc.* **2002**, *33*, 264–272.

- (20) Van den Brink, M.; German, A. L.; van Herk, A. M. On-line monitoring and control of the solution polymerization of n-butyl acrylate in dioxane by Raman spectroscopy. *Process Control Qual.* **1999**, *11*, 265–275.

- (21) van den Brink, M. On-Line Monitoring of Polymerization Reactions by Raman Spectroscopy: Application to Control of Emulsion Copolymerizations and Copolymerization Kinetics. Doctoral Thesis, Technische Universiteit Eindhoven, Eindhoven, The Netherlands, 2000.

- (22) Reis, M. M.; Uliana, M.; Sayer, C.; Araújo, P. H. H.; Giudici, R. Monitoring emulsion homopolymerization reactions using FT-Raman spectroscopy. *Braz. J. Chem. Eng.* **2005**, *22*, 61–74.
- (23) Santos, J. C.; Reis, M. M.; Machado, R. A. F.; Bolzan, A.; Sayer, C.; Giudici, R.; Araújo, P. H. H. Online Monitoring of Suspension Polymerization Reactions Using Raman Spectroscopy. *Ind. Eng. Chem. Res.* **2004**, *43*, 7282–7289.
- (24) Reis, M. M.; Araújo, P. H. H.; Sayer, C.; Giudici, R. Comparing near infrared and Raman spectroscopy for on-line monitoring of emulsion copolymerization reactions. *Macromol. Symp.* **2004**, *206*, 165–178.
- (25) Reis, M. M.; Araújo, P. H. H.; Sayer, C.; Giudici, R. Spectroscopic on-line monitoring of reactions in dispersed medium: chemometric challenges. *Anal. Chim. Acta* **2007**, *595*, 257–265.
- (26) Reis, M. M.; Araújo, P. H. H.; Sayer, C.; Giudici, R. Evidences of correlation between polymer particle size and Raman scattering. *Polymer* **2003**, *44*, 6123–6128.
- (27) Hergeth, W.-D. Raman Scattering on Polymeric Dispersions. *Chem. Eng. Technol.* **1998**, *21*, 647–651.
- (28) Elizalde, O.; Asua, J. M.; Leiza, J. R. Monitoring of emulsion polymerization reactors by Raman spectroscopy: calibration model maintenance. *Appl. Spectrosc.* **2005**, *59*, 1280–1285.
- (29) Wheaton, S.; Gelfand, R. M.; Gordon, R. Probing the Raman-active acoustic vibrations of nanoparticles with extraordinary spectral resolution. *Nat. Photonics* **2015**, *9*, 68–72.
- (30) Montagna, M. Brillouin and Raman scattering from the acoustic vibrations of spherical particles with a size comparable to the wavelength of the light. *Phys. Rev. B: Condens. Matter Mater. Phys.* **2008**, *77*, 045418.
- (31) Gouadec, G.; Colomban, P. Raman spectroscopy of nanomaterials: How spectra relate to disorder, particle size and mechanical properties. *Prog. Cryst. Growth Charact. Mater.* **2007**, *53*, 1–56.
- (32) Ito, K.; Kato, T.; Ona, T. Non-destructive method for the quantification of the average particle diameter of latex as water-based emulsions by near-infrared Fourier transform Raman spectroscopy. *J. Raman Spectrosc.* **2002**, *33*, 466–470.
- (33) Lin-Vien, D.; Colthup, N. B.; Fateley, W. G.; Grasselli, J. G. Alkanes. In *The Handbook of Infrared and Raman Characteristic Frequencies of Organic Molecules*; Lin-Vien, D., Colthup, N. B., Fateley, W. G., Grasselli, J. G., Eds.; Academic Press: San Diego, CA, 1991; Chapter 2, pp 9–28.
- (34) Reis, M. M.; Araujo, P. H. H.; Sayer, C.; Giudici, R. Development of calibration models for estimation of monomer concentration by Raman spectroscopy during emulsion polymerization: Facing the medium heterogeneity. *J. Appl. Polym. Sci.* **2004**, *93*, 1136–1150.
- (35) Hagiopol, C. (Georgia-Pacific Resins, Inc.). Styrene-acrylate copolymer composition suitable for surface size. U.S. Patent 6,734,232 B2, 2004.
- (36) Santos, A. M.; Coutinho, F. M. B. Effect of emulsifiers on emulsion copolymerization of styrene and n-butyl acrylate. *Polym. Bull.* **1993**, *30*, 407–414.
- (37) Cruz-Rivera, A.; Rios-Guerrero, L.; Monnet, C.; Schlund, B.; Guillot, J.; Pichot, C. Structure-property relationships in styrene-butyl acrylate emulsion copolymers: I. Preparation and characterization of latexes. *Polymer* **1989**, *30*, 1872–1882.
- (38) Chrástová, V.; Ďuračková, S.; Mrenica, J.; Ďernáková, L. Emulsifier and Initiator Effects on the Emulsion Copolymerization of Styrene with Butyl Acrylate. *Chem. Pap.* **1999**, *53*, 140–144.
- (39) Moffat, K. A.; Pontes, F. M.; Paine, A. J.; McAneney, B.; Puri, P. (Xerox Corporation). Styrene/n-butyl acrylate toner resins with excellent gloss and fix properties. U.S. Patent 5,462,828, 1995.
- (40) Lee, J.; Kim, S.; Yon, K. (Samsung Electronics Co., Ltd.). Preparation method of toner having micro radius. U.S. Patent 271970 A1, 2005.
- (41) Paine, A. J.; Pontes, F. M.; Moffat, K. A. (Xerox Corporation). Starve fed emulsion polymerization process. U.S. Patent 5,444,140, 1995.
- (42) Alsmeyer, F.; Koss, H.-J.; Marquardt, W. Indirect spectral hard modeling for the analysis of reactive and interacting mixtures. *Appl. Spectrosc.* **2004**, *58*, 975–985.
- (43) Ellis, G.; Claybourn, M.; Richards, S. E. The application of fourier transform raman spectroscopy to the study of paint systems. *Spectrochim. Acta Part A Mol. Spectrosc.* **1990**, *46*, 227–241.
- (44) Chu, B.; Fytas, G.; Zalczer, G. Study of thermal polymerization of styrene by Raman scattering. *Macromolecules* **1981**, *14*, 395–397.
- (45) Lamb, H. On the Vibrations of an Elastic Sphere. *Proc. London Math. Soc.* **1881**, *s1-13*, 189–212.
- (46) Reis, M. M.; Araújo, P. H. H.; Sayer, C.; Giudici, R. Correlation between Polymer Particle Size and in-situ NIR Spectra. *Macromol. Rapid Commun.* **2003**, *24*, 620–624.
- (47) Bastrukov, S. I. Low-frequency elastic response of a spherical particle. *Phys. Rev. E: Stat. Phys., Plasmas, Fluids, Relat. Interdiscip. Top.* **1994**, *49*, 3166–3170.